DOCK8 interference alleviates Aβ-induced damage of BV2 cells by inhibiting STAT3/NLRP3/NF-κB signaling

XUEYING ZHOU[1], JI HU[2], DEYI XU[1], SHENG ZHANG[1] and QIANYAN WANG[3]

Departments of [1]Psychiatry, [2]Anesthesiology and [3]Cardiology, Liyuan Hospital of Tongji Medical College, Huazhong University of Science and Technology, Wuhan, Hubei 430077, P.R. China

Received October 26, 2022; Accepted January 17, 2023

DOI: 10.3892/etm.2023.11833

Abstract. Dementia is defined as memory loss and other cognitive decline and it severely influences daily life. Alzheimer's disease (AD) is the most common cause of dementia. Dedicator of cytokinesis 8 (DOCK8) is reported to be involved in neurological diseases. The present study focused on investigating the role that DOCK8 serves in AD and addressing its hidden regulatory mechanism. Initially, $A\beta_{1-42}$ (Aβ) was applied for the administration of BV2 cells. Subsequently, the mRNA and protein expression levels of DOCK8 were evaluated utilizing reverse transcription-quantitative PCR (RT-qPCR) and western blotting. After the DOCK8 silencing, immunofluorescence staining (IF), ELISA, wound healing and Transwell assays were applied to assess ionized calcium binding adapter molecule-1 (IBA-1) expression, release of inflammatory factors, migration and invasion in Aβ-induced BV2 cells. IF was used to evaluate cluster of differentiation (CD)11b expression. RT-qPCR and western blotting were to analyze the levels of M1 cell markers inducible nitric oxide synthase (iNOS) and CD86. The expression of STAT3/NLR family pyrin domain containing 3 (NLRP3)/NF-κB signaling-related proteins were determined by western blotting. Finally, the viability and apoptosis in hippocampal HT22 cells with DOCK8 depletion were estimated. Results revealed that Aβ induction greatly stimulated the expression levels of IBA-1 and DOCK8. DOCK8 silencing suppressed Aβ-induced inflammation, migration and invasion of BV2 cells. Additionally, DOCK8 deficiency conspicuously decreased the expression levels of CD11b, iNOS and CD86. The expression of phosphorylated (p-)STAT3, NLRP3, ASC, caspase1 and p-p65 was downregulated in Aβ-induced BV2 cells after DOCK8 depletion. STAT3 activator Colivelin reversed the effects of DOCK8 knockdown on IBA-1 expression, inflammation, migration, invasion and M1 cell polarization. In addition, the viability and apoptosis in hippocampal HT22 cells stimulated by neuroinflammatory release of BV2 cells were repressed following DOCK8 deletion. Collectively, DOCK8 interference alleviated Aβ-induced damage of BV2 cells by inhibiting STAT3/NLRP3/NF-κB signaling.

Correspondence to: Dr Qianyan Wang, Department of Cardiology, Liyuan Hospital of Tongji Medical College, Huazhong University of Science and Technology, 39 Lake Avenue, Wuchang, Wuhan, Hubei 430077, P.R. China
E-mail: wangqianyan_1122@163.com

Key words: dedicator of cytokinesis 8, inflammation, Alzheimer's disease, STAT3, NF-κB

Introduction

Dementia, which features memory loss and cognitive decline, severely influences daily life (1). As a most common contributor to dementia, Alzheimer's disease (AD) accounts for 50-75% of dementia cases (2). AD, which is a common progressive neurodegenerative disease, features the formation of extracellular amyloid plaques as well as intracellular neurofibrillary tangles (3). An increasing number of researches have shown that the neuroinflammation of AD has a close association with neurological dysfunction, which is mediated by the progressive activation of glial cells and the consequent overproduction of pro-inflammatory cytokines (4,5). In AD, neuroinflammation acts as a major element in disease advancement, which features the activities of brain resident glial cells, particularly microglia (6). The over-activated microglia can promote the release of inflammatory cytokines, chemokines, and oxygen/nitrogen radicals, thereby exacerbating the neuronal damage (7,8).

The dedicator of cytokinesis (DOCK) proteins, which are the members of the family of atypical guanine exchange factors, can trigger ϱGTPases Rac1 and/or Cdc42 and serve as critical players in cellular activities, such as cell migration, neuronal polarization as well as neuroprotection (9). DOCK8, which belongs to DOCK family of proteins, is highly expressed in B cells as well as T cells and has been widely investigated in immune system (9,10). In addition, DOCK8 exists in microglia and can regulate the advancement of neurodegenerative diseases (11). The depletion of DOCK8 imparts alleviative effects on the migration and function of immune cells (12). DOCK2, another member of DOCK family of proteins, is involved with the advancement of AD (13,14). Nevertheless, the role that DOCK8 played in AD remains to be elucidated.

In the present study, $A\beta_{1-42}$ (Aβ) was used for the stimulation of BV2 cells to induce inflammatory damage.

The present study was performed to discuss the role of DOCK8 in Aβ-induced BV2 cells and to elucidate its hidden regulatory mechanism in alleviating hippocampal neuronal damage.

Materials and methods

Cell culture and treatment. BV2 microglia cells and hippocampal HT22 cells provided by Shanghai Hongshun Biotechnology Co., Ltd were cultivated in modified Eagle's medium (MEM; Thermo Fisher Scientific, Inc.) which contained 10% fetal bovine serum (FBS; Guangzhou Perseco Biotechnology Co., Ltd.) and 1% penicillin/streptomycin and were placed in a humid atmosphere at 37˚C in the presence of 5% CO_2. To stimulate inflammatory damage, 10 μM Aβ oligomers (GL Biochem) was administered to BV2 cells for 24 h at 37˚C and the culture medium was considered as conditioned medium (CM) (1). With the purpose of further discovering the mechanism of DOCK8 in STAT3 signaling, STAT3 activator Colivelin (0.5 μM) was applied to BV2 cells with Aβ induction (15). To activate HT22 cells, cells were plated in 96-well plates (1.5 x10^4/well) in serum-free culture medium were treated with BV2 CM for 24 h at 37˚C (16).

Cell transfection. To deplete DOCK8 expression, 100 nM small interfering RNAs (siRNA) specific to DOCK8 (siRNA-DOCK8-1, CGGAAAAACCAAGGAAGTTCAGA; siRNA-DOCK8-2, CTCTGAAGTTTGAGATTGAAATT) as well as its negative control (siRNA-NC, CCCGATTTCCGA GAATTCTCATTCA) provided by Shanghai GeneChem Co., Ltd. were transfected into BV2 cells or HT22 cells seeded into 6-well plates (2x10^5 cells/well) using Lipofectamine® 3000 (Invitrogen; Thermo Fisher Scientific, Inc.) for 48 h at 37˚C according to the manufacturer's protocols. At 48 h following transfection, the transfection efficacy was tested with reverse transcription-quantitative polymerase chain reaction (RT-qPCR).

Immunofluorescence (IF) staining. Following Aβ induction, BV2 cells were subjected to 4% paraformaldehyde for 20 min at room temperature and 0.2% Triton X-100 permeation for 20 min at room temperature. Subsequently, the PBS-rinsed cells were blocked with 1% bovine serum albumin at room temperature. The overnight exposure of cells to primary antibodies targeting IBA-1 (ab178846; 1:500; Abcam) and CD11b (ab184308; 1:500; Abcam) was performed at 4˚C, followed by probing with rabbit anti-mouse IgG H&L (ab6728; 1:1,000; Abcam) at 37˚C for 30 min. After nuclear staining with DAPI (Shenzhen Ziker Biotechnology Co., Ltd.) for 10 min at room temperature, a fluorescence microscope (Olympus Corporation) was used to capture images.

Enzyme-linked immunosorbent assay (ELISA). Using ELISA kits (Shanghai Xitang Biotechnology, China), the levels of inflammatory cytokines TNF-α (cat. no. F11630), IL-1β (cat. no. F10770) and IL-6 (cat. no. F10830) in cell supernatants were detected according to the manufacturer's protocols. Optical density (OD) value was resolved at λ=450 nm using a microplate reader (Molecular Devices, LLC). The results were calculated according to the standard curve.

Wound healing assay. The migrative capability of Aβ-induced BV2 cells was assessed using wound healing assay. Initially, BV2 cells were cultured in 6-well plates using serum-free medium until 95% confluence was achieved. Thereafter, a wound in the cell monolayer was created with a 10-μl pipette tip. The BV2 cells were rinsed with PBS and cultured at 37˚C in the presence of 5% CO_2. At 0 and 24 h, images of the wound areas were captured by a light microscope (Olympus Corporation). Image J software (Version 1.52r; National Institutes of Health) was used to visualize the of migrative cells.

Transwell assay. The invasive capability of Aβ-induced BV2 cells was estimated using Transwell assay. The upper compartment of the Transwell was coated with Matrigel (BD Biosciences) at 37˚C for 30 min and used for BV2 cells. Medium, with 10% FBS, was added to the low chamber. Invaded BV2 cells were fixed with 4% paraformaldehyde for 30 min and stained with 0.1% crystal violet for 20 min at room temperature. The area of invaded cells was tracked using a light microscope (Olympus Corporation).

Cell Counting Kit-8 (CCK-8) assay. BV2 cells in 96-well plates were cultured for 24 h at 37˚C. CCK-8 reagent (10 μl; Beyotime Institute of Biotechnology) was added and the cells cultured for another 2 h at 37˚C. A microplate reader (Molecular Devices, LLC) was used to assess absorbance at 450 nm.

Terminal-deoxynucleotidyl transferase mediated nick end labeling (TUNEL). The apoptosis level of BV2 cells was assessed using TUNEL staining (Beyotime Institute of Biotechnology). Paraformaldehyde (4%) and Triton X-100 (0.5%) was used to treat BV2 cells for 15 and 20 min respectively at room temperature. Subsequently, the cells were labeled with TUNEL for 1 h at 37˚C. The counterstaining of cells with 1 μg/ml DAPI was performed at 37˚C for 30 min in the dark. The observation of positive cells in five randomly selected fields was performed under a florescent microscope (Olympus Corporation).

RT-qPCR. Total RNA was isolated from sample cells placed in a 6-well plate (6x10^4 cells/well) with TRIzol® reagent (Thermo Fisher Scientific, Inc.) according to the manufacturer's protocols and reverse transcribed into cDNA using the RevertAid cDNA Synthesis kit (Beijing Zhijie Fangyuan Technology Co., Ltd.) according to the manufacturer's protocols. PCR reactions were performed using iTaq Universal SYBR Green kit (Bio-Rad Laboratories, Inc.) on the MX3000p PCR system (Agilent Technologies, Inc.) according to the manufacturer's protocols. RT-qPCR was performed at 50˚C for 2 min and 95˚C for 2 min, followed by 40 cycles at 95˚C for 15 sec and 60˚C for 1 min. The calculation of relative gene expression was operated with the $2^{-\Delta\Delta Cq}$ (17). The primer sequences were: DOCK8 forward primer: 5'-GGCTGACAGATGAGGCTG G-3', reverse primer: 5'-TCAAAGTCCACTGGCTCGAC-3'; inducible nitric oxide synthase (iNOS) forward primer: 5'-AGG GCCACCTCTACATTTGC-3', reverse primer: 5'-CCCAAG CCATCATTGGGAGT-3'; CD86 forward primer: 5'-TCAATG GGACTGCATATCTGCC-3', reverse primer: 5'-GCCAAA

ATACTACCAGCTCACT-3' or GAPDH forward primer: 5'-GCCTCCTCCAATTCAACCCT-3', reverse primer: 5'-CTC GTGGTTCACACCCATCA-3'. GAPDH was designated as a standard internal control for relative gene expression. This experiment was repeated three times.

Western blotting. Total proteins were isolated from samples with RIPA lysis buffer (Beyotime Institute of Biotechnology), after which was the concentration quantification applying a bicinchoninic acid (protein assay kit (Shanghai Yisheng Biotechnology Co., Ltd.). The proteins (30 μg) were separated by 8% SDS-PAGE, transferred to PVDF membranes and blocked by 5% non-fat milk at room temperature for 1 h. Subsequently, the overnight cultivation of membranes with primary antibodies was performed at 4˚C, after which was the probe with HRP-labeled rabbit anti-mouse secondary antibody (cat. no. 7074P2; 1:5,000; Cell Signaling Technology, Inc.) at room temperature for 2 h. Finally, the visualization and analysis of protein blots were performed with ECL (Yeasen Biotech) and ImageJ (Version 1.52r; National Institutes of Health). GAPDH was used as the loading control. The following primary antibodies were used: anti-DOCK8 (cat. no. 39263S; 1:1,000), anti-CD86 (cat. no. 19589S; 1:1,000), anti-iNOS (cat. no. 13120S; 1:1,000), anti-NOD-like receptor family pyrin domain containing 3 (NLRP3; cat. no. 15101S; 1:1,000), anti-apoptosis-associated speck-like protein containing a caspase recruitment domain (ASC; cat. no. 67824T; 1:1,000), anti-caspase1 (cat. no. 24232S; 1:1,000), anti-p-p65 (cat. no. 3033T; 1:1,000), anti-p65 (cat. no. 8242T; 1:1,000), anti-Bcl2 (cat. no. 3498T; 1:1,000), anti-Bax (cat. no. 14796S; 1:1,000), anti-cleaved caspase3 (cat. no. 9664T; 1:1,000), anti-caspase3 (cat. no. 9662S; 1:1,000) and anti-GAPDH (cat. no. 5174T; 1:1,000) antibodies were from by Cell Signaling Technology, Inc. Anti-p-STAT3 (cat. no. ab76315; 1:2,000) and anti-STAT3 (cat. no. ab68153; 1:2,000) antibodies were purchased from Abcam.

Statistical analysis. Data were given as mean ± standard deviation (SD) and were analyzed using GraphPad Prism 8.0 software (Dotmatics). One-way ANOVA and Tukey's post-hoc test was used for comparisons between multiple groups. $P<0.05$ was considered to indicate a statistically significant difference.

Results

DOCK8 expression increases in Aβ-induced BV2 cells. Initially, Aβ was used for the induction of BV2 cells and IF adopted to analyze IBA-1 expression. Compared with the Control group, Aβ induction elevated IBA-1 expression in BV2 cells in a time-dependent manner (Fig. 1A). Results obtained from RT-qPCR and western blotting demonstrated that the mRNA and protein expression levels of DOCK8 in BV2 cells were enhanced by Aβ stimulation compared with the Control group (Fig. 1B and C). It was evident that DOCK8 was increased in Aβ-induced BV2 cells.

DOCK8 interference inhibits the activation and inflammatory factors release of Aβ-induced BV2 cells. To decrease DOCK8 expression, siRNAs specific to DOCK8 were transfected into BV2 cells and then RT-qPCR was used to the test transfection efficacy. As shown in Fig. 2A, the expression of DOCK8 in BV2 cells declined after transfection with siRNA targeting DOCK8 when compared to the Control group. Notably, DOCK8 had lower expression in siRNA-DOCK8-2 group than that in siRNA-DOCK8-1 group, thus siRNA-DOCK8-2 was adopted the following experiments. Compared with the Control group, Aβ stimulation markedly increased IBA-1 expression, which was then decreased by DOCK8 interference (Fig. 2B). In addition, the increased levels of TNF-α, IL-6 and IL-1β in BV2 cells caused by Aβ induction were decreased after decreasing DOCK8 expression (Fig. 2C), suggesting that DOCK8 silence imparted a suppressive effect on the inflammatory response of Aβ-induced BV2 cells.

DOCK8 interference inhibits the migration and invasion of Aβ-induced BV2 cells. In contrast to the Control group, the migrative ability of BV2 cells was markedly increased by Aβ stimulation. Nevertheless, DOCK8 silencing imparted suppressive effects on the migration of Aβ-induced BV2 cells, as evidenced by reduced migrative ability in the Aβ + siRNA-DOCK8 group compared with the Aβ + siRNA-NC group (Fig. 3A). Additionally, the enhanced invasion of Aβ-induced BV2 cells subsequently declined following siRNA DOCK8 expression (Fig. 3B). The above results demonstrated that DOCK8 interference inhibited the migration and invasion of Aβ-induced BV2 cells.

DOCK8 interference inhibits the polarization of Aβ-induced BV2 cells to M1 cells. Results from IF staining showed that Aβ stimulation conspicuously increased the level of CD11b compared with that in the Control group while DOCK8 deficiency showed opposite effects on this protein, evidenced by reduced CD11b content in Aβ + siRNA-DOCK8 in comparison with that in Aβ + siRNA-NC group (Fig. 4A). Elsewhere, the expression levels of iNOS and CD86 in BV2 cells assessed with RT-qPCR and western blotting were notably elevated by Aβ induction and then reduced following interfering DOCK8 expression (Fig. 4B and C). Collectively, DOCK8 interference inhibited the polarization of Aβ-induced BV2 cells to M1 cells.

DOCK8 interference inhibits STAT3/NLRP3/NF-κB signal in Aβ-induced BV2 cells. Compared with the Control group, Aβ induction remarkably increased the expression of p-STAT3, NLRP3, ASC, caspase1 and p-p65. Nonetheless, DOCK8 depletion decreased the contents of the above proteins in Aβ-induced BV2 cells when compared to the Aβ + siRNA-NC group (Fig. 5). Notably, both Aβ induction and DOCK8 silencing had no significant effects on the contents of STAT3 and p65. The above results suggested that DOCK8 interference inhibited the STAT3/NLRP3/NF-κB signaling pathway in Aβ-stimulated BV2 cells.

DOCK8 interference inhibits the activation and release of inflammatory factors in Aβ-induced BV2 cells via inactivation of STAT3/NLRP3/NF-κB pathway. To further investigate the mechanism of DOCK8 in STAT3 signal, Colivelin, which is an activator of STAT3, was administered to BV2 cells. Results obtained from western blotting

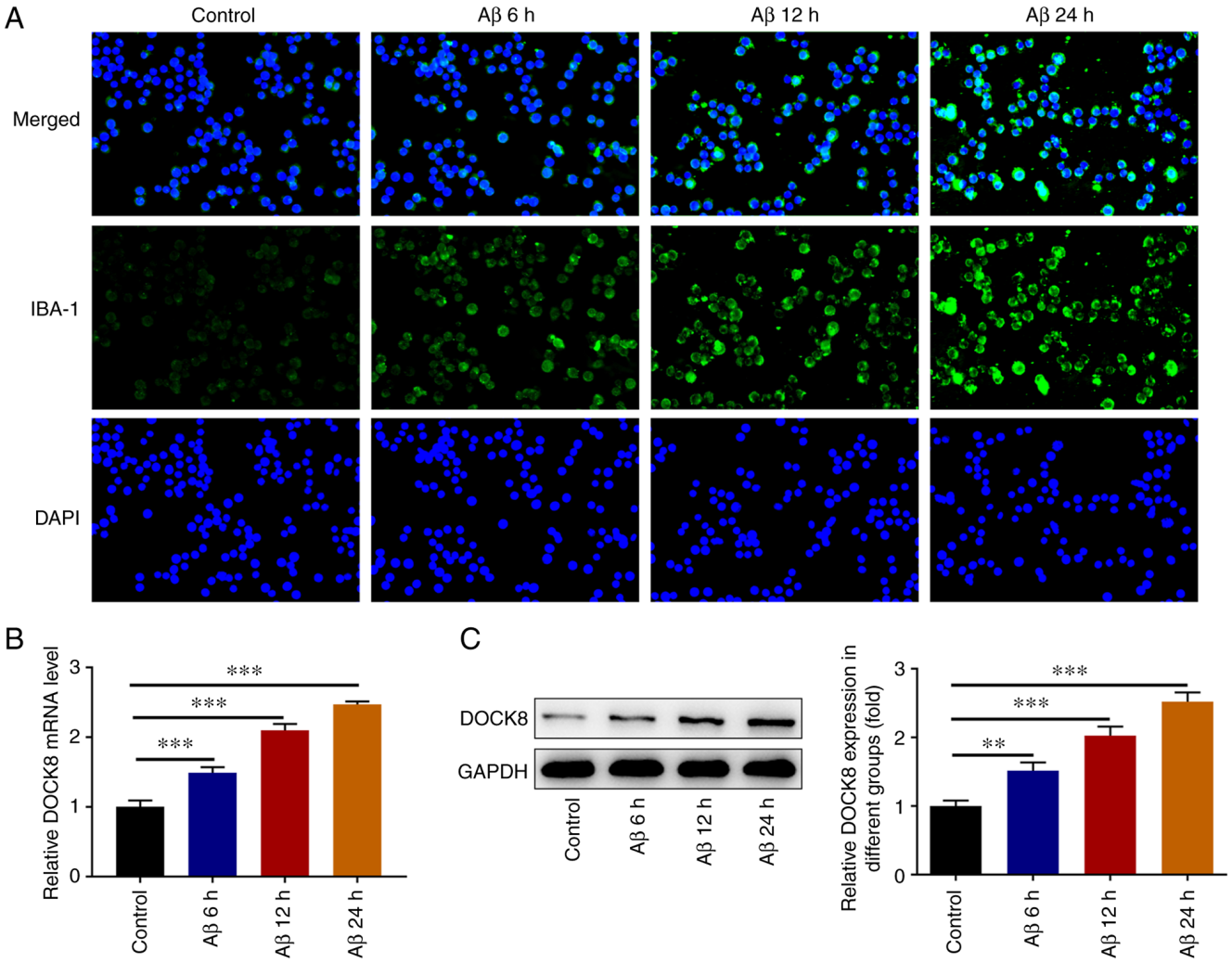

Figure 1. DOCK8 expression is increased in Aβ-induced BV2 cells. (A) The expression of IBA-1 was detected using IF staining. Magnification, x200. The mRNA and protein expression levels of DOCK8 were detected using (B) Reverse transcription-quantitative PCR and (C) western blotting. **P<0.01 and ***P<0.001 vs. control. DOCK8, dedicator of cytokinesis 8; Aβ, amyloid β.

showed that the decreased contents of p-STAT3, NLRP3, ASC, caspase1 and p-p65 in Aβ-induced BV2 cells caused by DOCK8 interference were partially elevated after administration with Colivelin (Fig. 6A). Compared with the Aβ group, the expression of IBA-1 was decreased after depleting DOCK8 expression and was subsequently rescued by Colivelin administration (Fig. 6B). Furthermore, DOCK8 interference decreased the levels of TNF-α, IL-1β and IL-6 in Aβ-induced BV2 cells compared with the Aβ group while Colivelin exhibited opposite effects on these inflammatory cytokines, as testified by increased levels of TNF-α, IL-1β and IL-6 in Aβ + siRNA-DOCK8+STAT3 activator group (Fig. 6C). To conclude, DOCK8 interference suppressed the activation and inflammation of Aβ-induced BV2 cells by blocking STAT3/NLRP3/NF-κB pathway.

DOCK8 interference inhibits the migration and invasion of Aβ-induced BV2 cells by suppressing STAT3/NLRP3/NF-κB pathway. In comparison with the Control group, Aβ induction markedly increased the migrative ability of BV2 cells, which then declined following transfection of cells with siRNA targeting DOCK8 (Fig. 7A). Nevertheless, the decreased migration in Aβ-induced BV2 cells was quickly enhanced by Colivelin administration, revealing that DOCK8 depletion suppressed the migrative capability of Aβ-induced BV2 cells via inhibiting STAT3 signal. Similarly, the reduced invasive ability of Aβ-induced BV2 cells was also increased after treating cells with Colivelin (Fig. 7B).

DOCK8 interference inhibits the polarization of Aβ-induced BV2 cells to M1 cells by restraining STAT3/NLRP3/NF-κB pathway. Evidently, the reduced CD11b level in Aβ-induced BV2 cells that resulted from DOCK8 interference was elevated by Colivelin compared with that in Aβ + siRNA-DOCK8 group (Fig. 8A). Similarly, DOCK8 deficiency decreased the contents of CD86 and iNOS in Aβ-induced BV2 cells compared with the Aβ group and these were subsequently increased by Colivelin treatment (Fig. 8B and C). In summary, DOCK8 silencing repressed the polarization of Aβ-induced BV2 cells to M1 cells via blocking the STAT3/NLRP3/NF-κB pathway.

DOCK8 interference inhibits the neuronal activity damage and apoptosis of hippocampal HT22 cells induced by

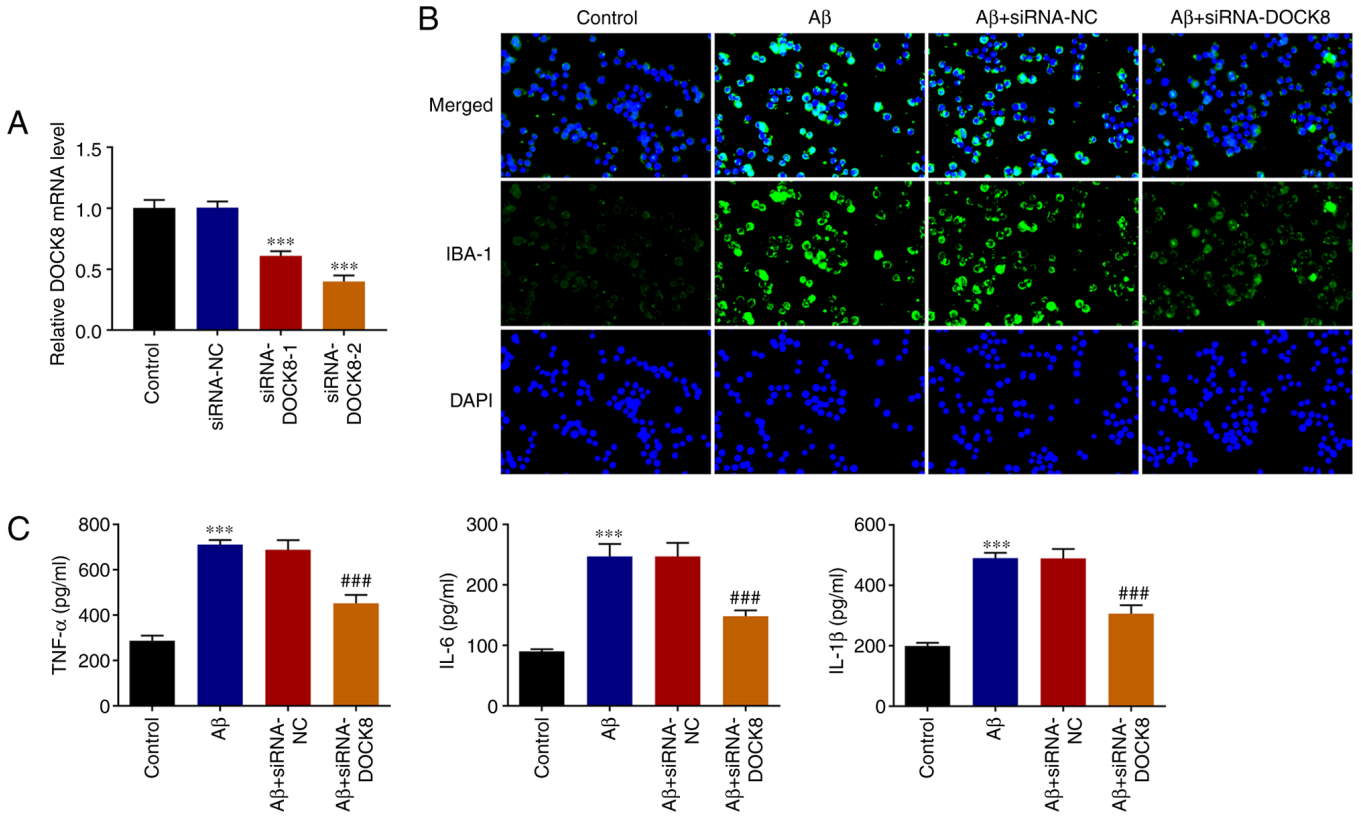

Figure 2. DOCK8 interference inhibits the activation and inflammatory factors release of Aβ-induced BV2 cells. (A) The transfection efficacy was detected using reverse transcription-quantitative PCR. ***P<0.001 vs. siRNA-NC. (B) The expression of IBA-1 in transfected cells was detected using immunofluorescence staining. Magnification, x200. (C) The levels of inflammatory cytokines were detected using ELISA. ***P<0.001 vs. control; ###P<0.001 vs. Aβ + siRNA-NC. DOCK8, dedicator of cytokinesis 8; Aβ, amyloid β; siRNA, short interfering RNA; NC, negative control; IBA-1, ionized calcium binding adapter molecule-1.

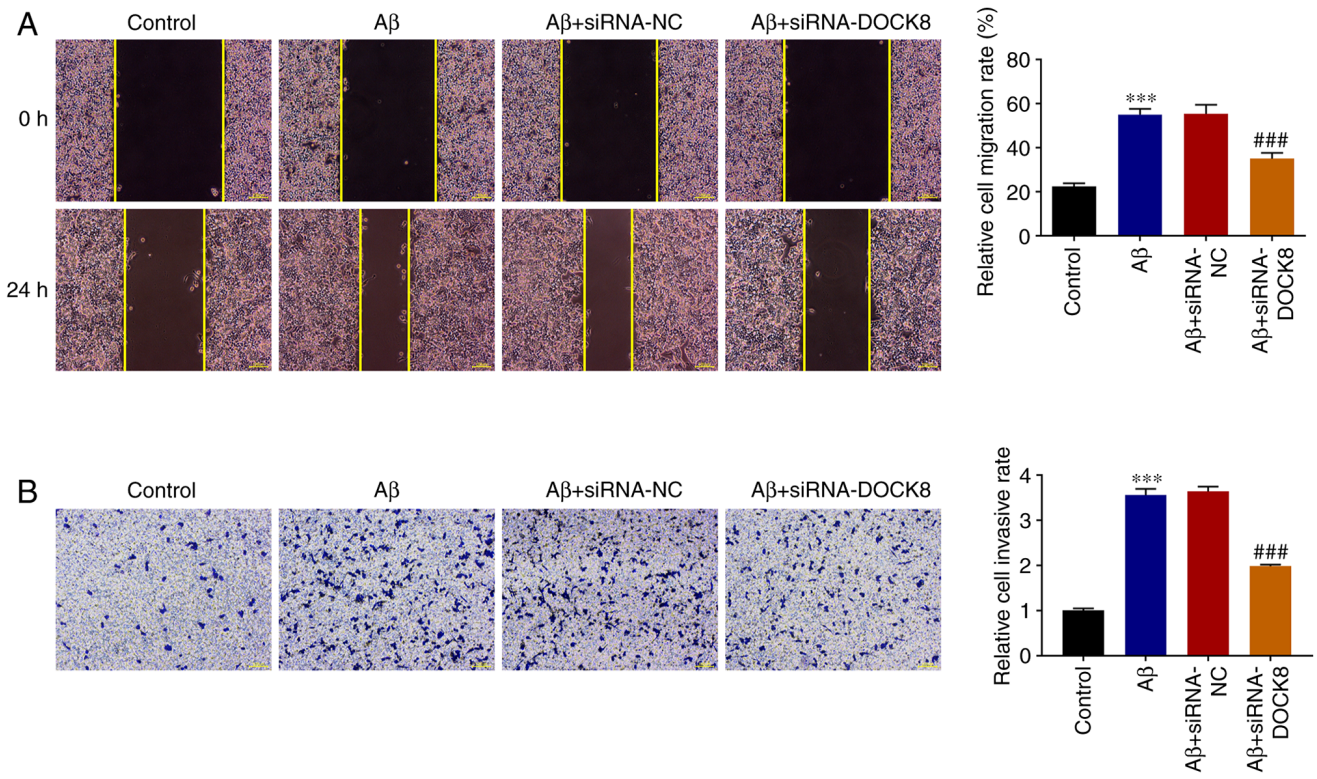

Figure 3. DOCK8 interference inhibits the migration and invasion of Aβ-induced BV2 cells. (A) The migration was detected using wound healing assay. Magnification, x100. (B) The invasion was detected using Transwell assay. Magnification, x100. ***P<0.001 vs. control; ###P<0.001 vs. Aβ + siRNA-NC. DOCK8, dedicator of cytokinesis 8; Aβ, amyloid β; siRNA, short interfering RNA; NC, negative control.

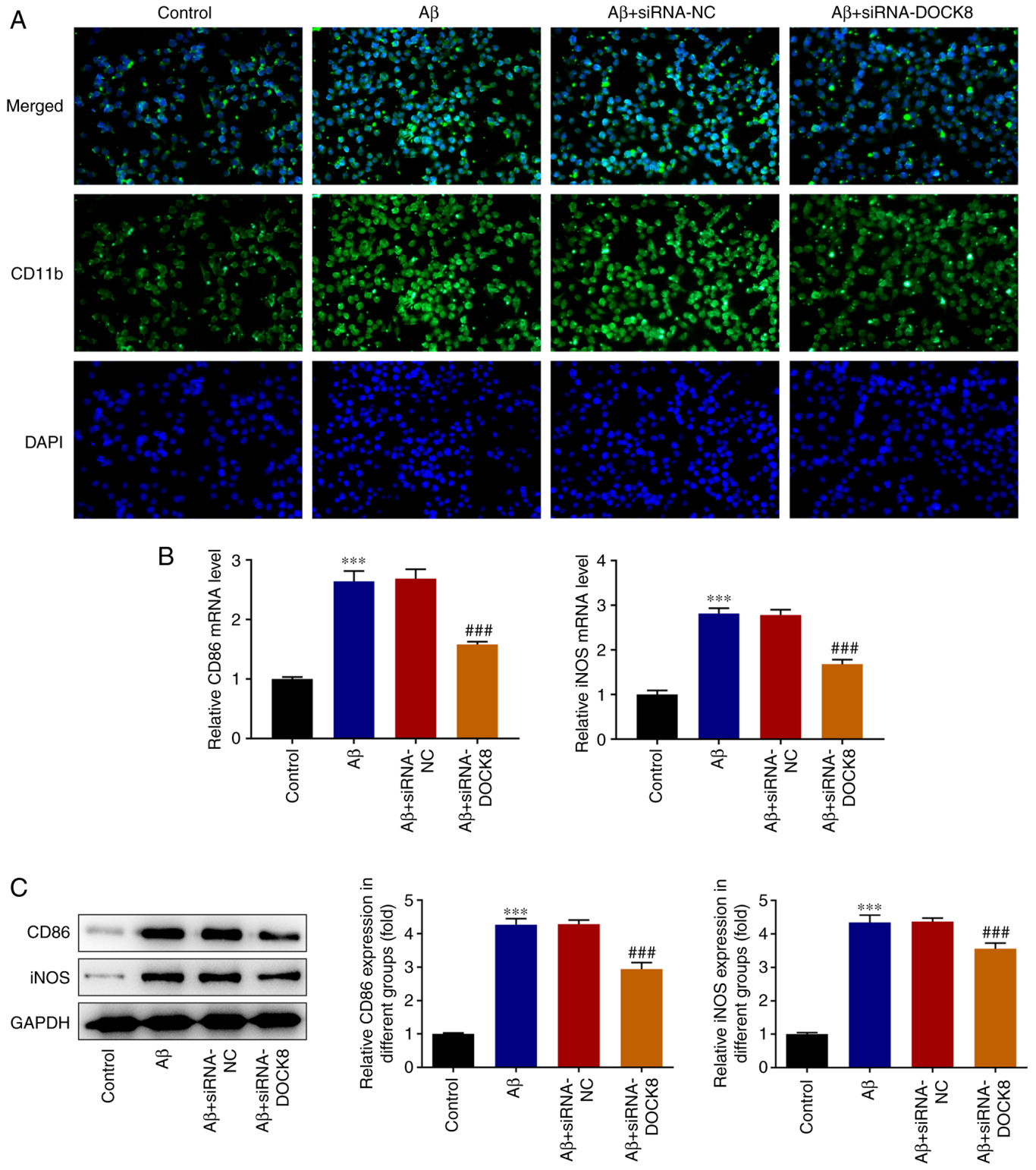

Figure 4. DOCK8 interference inhibits the polarization of Aβ-induced BV2 cells to M1 cells. (A) The expression of CD11b was detected using immunofluorescence staining. Magnification, x200. The expression levels of iNOS and CD86 using (B) reverse transcription-quantitative PCR and (C) western blotting. ***P<0.001 vs. control; ###P<0.001 vs. Aβ + siRNA-NC. DOCK8, dedicator of cytokinesis 8; Aβ, amyloid β; CD, cluster of differentiation; iNOS, inducible nitric oxide synthase; siRNA, short interfering RNA; NC, negative control.

neuroinflammatory release in BV2 cells. As observed from Fig. 9A, hippocampal HT22 cells transfected with siRNA-DOCK8-1/2 presented significantly downregulated DOCK8 expression compared with the siRNA-NC group. SiRNA-DOCK8-2 was selected to perform the subsequent experiments due to the lower DOCK8 expression in HT22 cells. As Fig. 9B showed, Aβ stimulation reduced the viability of HT22 cells compared with the Control group. Nonetheless, the declined viability of Aβ-induced HT22 cells was rapidly revived after the cells were transfection with siRNA-DOCK8.

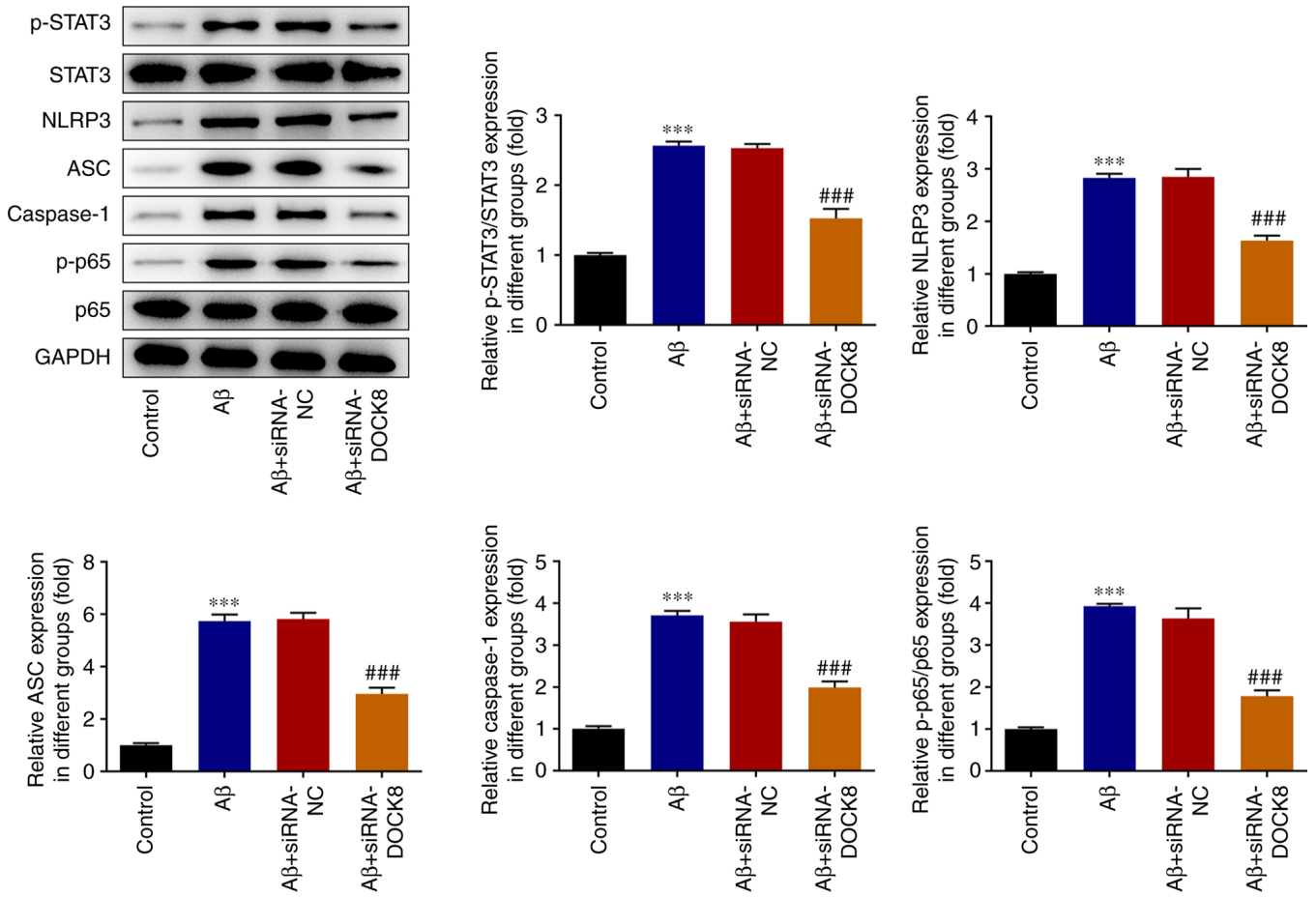

Figure 5. DOCK8 interference inhibits STAT3/NLRP3/NF-κB signaling in Aβ-induced BV2 cells. The expression levels of STAT3, p-STAT3, NLRP3, ASC, caspase1, p-p65 and p65 were detected using western blotting. ***P<0.001 vs. control; ###P<0.001 vs. Aβ + siRNA-NC. DOCK8, dedicator of cytokinesis 8; NLRP3, NLR family pyrin domain containing 3; Aβ, amyloid β; p-, phosphorylated; siRNA, short interfering RNA; NC, negative control.

Apoptosis was appraised by TUNEL and the results demonstrated that Aβ stimulation conspicuously enhanced the apoptosis level of HT22 cells compared with the Control group, which was subsequently notably diminished by DOCK8 interference (Fig. 9C and D). Moreover, Aβ stimulation decreased Bcl2 content but markedly increased the contents of Bax and cleaved caspase3 compared with the Control group, while DOCK8 depletion exhibited opposite effects on these proteins, evidenced by elevated Bcl2 content as well as diminished contents of Bax and cleaved caspase3 in Aβ + siRNA-DOCK8 group (Fig. 9E).

Discussion

Extensive studies evidence that neuroinflammation acts as a predominant player in the pathogenesis of AD as well as other neurodegenerative disorders (4,18,19). Accumulated Aβ deposition can be a marker of AD and the aggregation of Aβ peptide can trigger microglia (19). In addition, the triggered microglia can stimulate inflammatory response including the secretion of inflammatory factors, thereby contributing to brain damage (20). IBA-1, which is a microglia/macrophage-specific marker, has been broadly used for microglial assessment (21-23). IBA-1 is increased in activated microglia (24,25), which indicates that the upregulation of IBA-1 could serve as a hallmark for microglial activation (26,27). Therefore, the present study used Aβ to stimulate BV2 microglia cells to induce inflammatory damage *in vitro* and then used IF staining to resolve the expression of IBA-1. It was discovered that Aβ induction elevated the level of IBA-1, suggesting the activation of BV2 cells, which was consistent with the findings in aforementioned studies.

DOCK8, which is located on chromosome 9p24.3, is reported to be expressed in microglia (28). Previous researches have verified that DOCK8 exhibits the feature of autoimmunity and serves as an indispensable role in immune surveillance (29,30). In addition, DOCK8 has been widely considered in neurodegenerative diseases. Taking glaucoma as an instance, DOCK8 exhibits existence in microglia and mediates microglial activity in the process of neurodegeneration (11). Additionally, Xu *et al* (31) suggest that DOCK8 is conspicuously increased in patients suffering from multiple sclerosis. DOCK8 is acknowledged to be a critical regulator in cell migration, invasion, survival, inflammation as well as polarization. For example, the interference of DOCK8 can suppress the migrative ability of PDGF-induced Schwann cell precursor (32). A previous study demonstrated that depleted DOCK8 contributed to decreased polarization (33). Although numerous researches

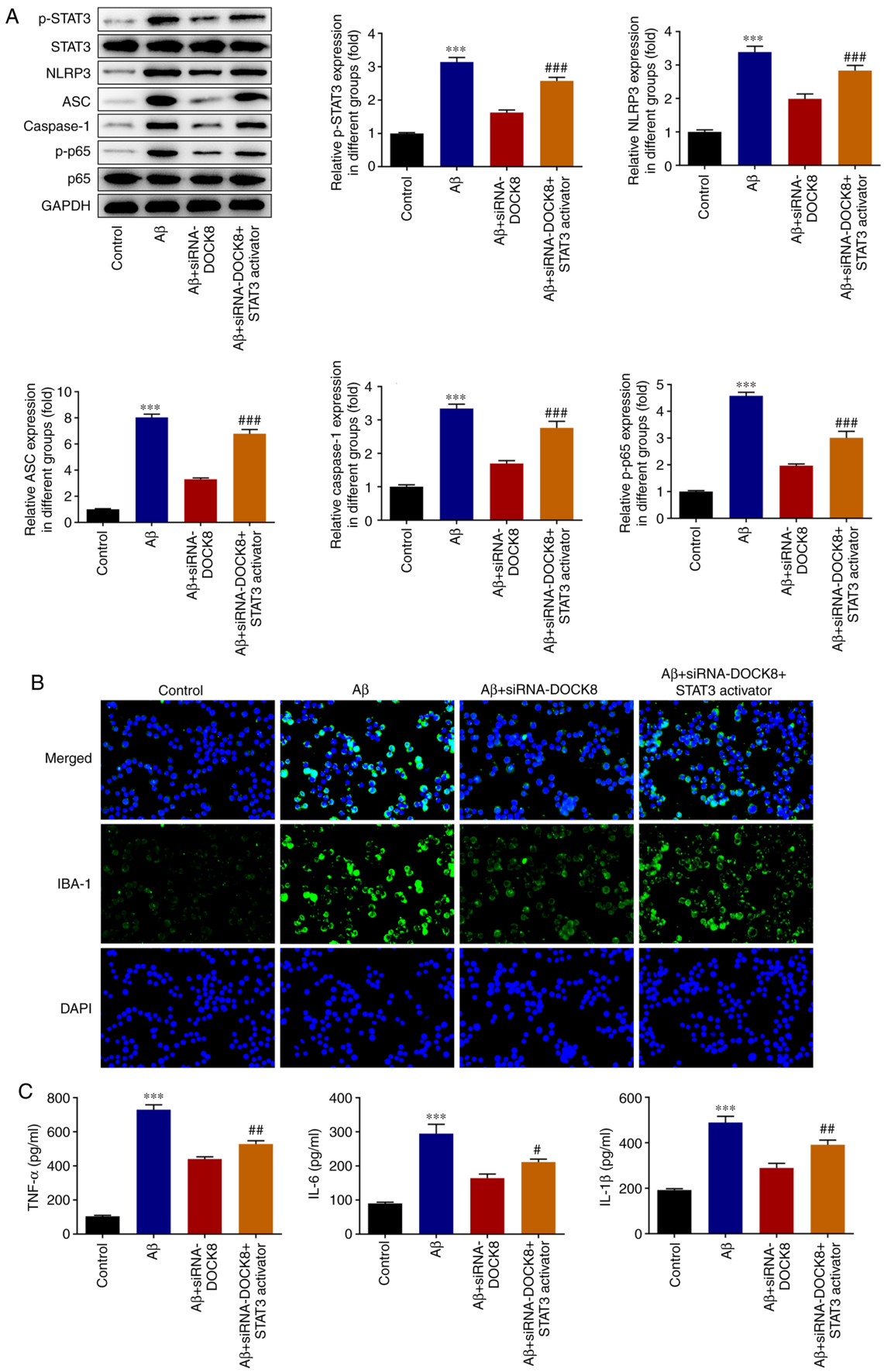

Figure 6. DOCK8 interference inhibits the activation and inflammatory factors release of Aβ-induced BV2 cells by suppressing STAT3/NLRP3/NF-κB signaling. (A) The expression levels of STAT3, p-STAT3, NLRP3, ASC, caspase1, p-p65 and p65 were detected using western blotting. (B) The expression of IBA-1 was detected using immunofluorescence staining. Magnification, x200. (C) The levels of inflammatory cytokines were detected using ELISA. ***P<0.001 vs. control; $^{\#}$P<0.05, $^{\#\#}$P<0.01, $^{\#\#\#}$P<0.001 vs. Aβ + siRNA-DOCK8. DOCK8, dedicator of cytokinesis 8; Aβ, amyloid β; NLRP3, NLR family pyrin domain containing 3; p-, phosphorylated; siRNA, short interfering RNA; NC, negative control; IBA-1, ionized calcium binding adapter molecule-1.

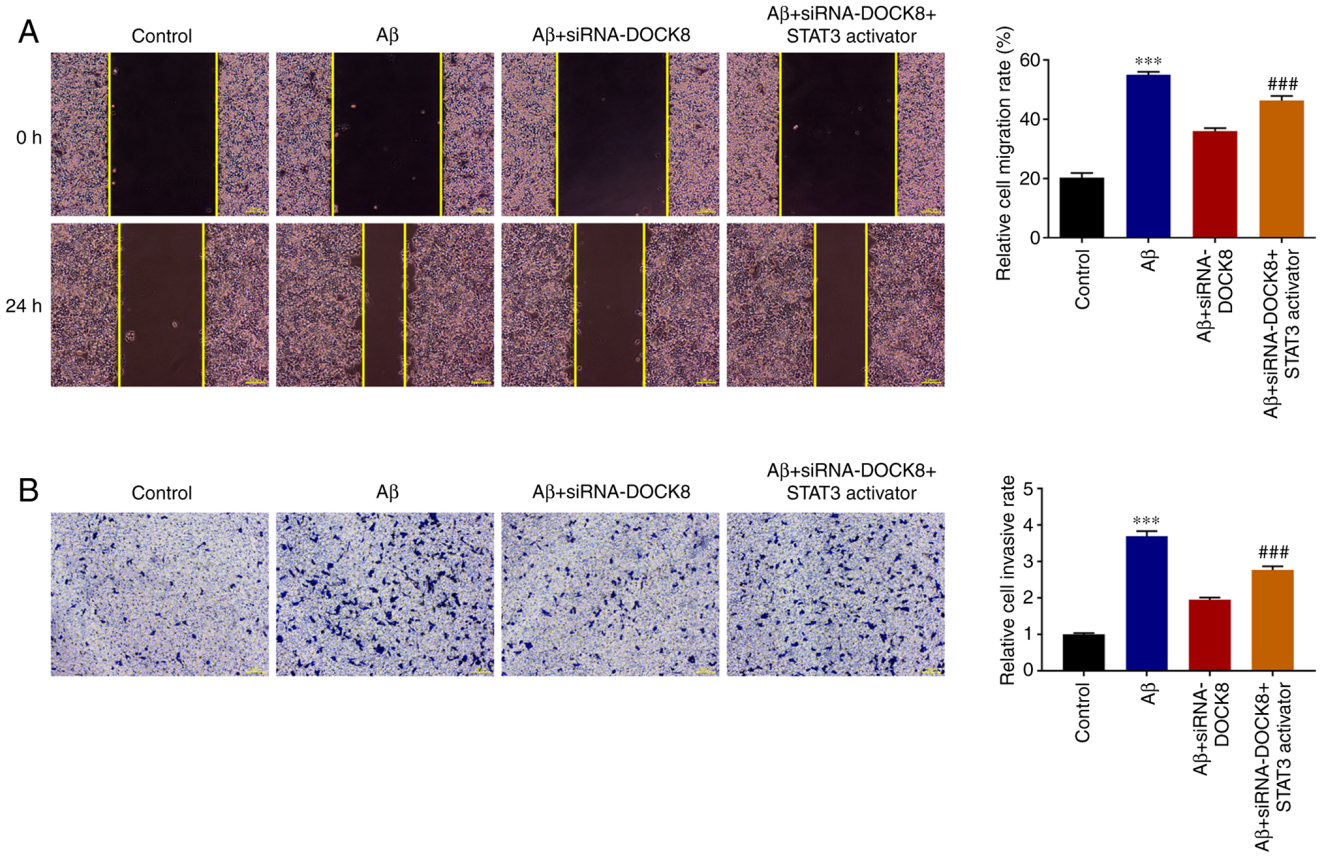

Figure 7. DOCK8 interference inhibits the migration and invasion of Aβ-induced BV2 cells by suppressing STAT3/NLRP3/NF-κB signaling. (A) The cell migration was detected using wound healing assay. Magnification, x100. (B) The cell invasion was detected using Transwell assay. Magnification, x100. ***P<0.001 vs. control; ###P<0.001 vs. Aβ + siRNA-DOCK8. DOCK8, dedicator of cytokinesis 8; Aβ, amyloid β; NLRP3, NLR family pyrin domain containing 3; siRNA, short interfering RNA; NC, negative control.

have been performed (11,31-33), the role that DOCK8 played in AD has not yet been elucidated. In the present study, the mRNA and protein expression levels of DOCK8 in BV2 cells were notably increased following Aβ stimulation, revealing the upregulation of DOCK8 in AD. After silencing DOCK8, a series of functional experiments were performed. The increased expression of IBA-1 in Aβ-induced BV2 cells was downregulated following silencing DOCK8, revealing that DOCK8 deficiency suppressed the activation of BV2 cells with Aβ stimulation. In addition, DOCK8 silencing also imparted suppressive effects on the inflammation, migration and invasion of Aβ-stimulated BV2 cells. Elsewhere, the decreased contents of CD11b, CD86 and iNOS in DOCK8-silenced BV2 cells with Aβ stimulation implied that DOCK8 interference repressed the polarization of Aβ-induced BV2 cells to M1 cells.

On the basis of size similarity, antigenic as well as structural relatedness, STAT3 is identified as belonging to the STAT family (34). It is reported that STAT3 possesses an anti-inflammatory property and can mediate crucial cellular activities, such as cell growth, apoptosis and transcription of inflammatory genes (35,36). Additionally, the dysregulation of STAT3 is involved with the advance of numerous malignancies and neurodegenerative diseases (37). STAT3 signaling can be activated in Aβ-induced microglia (38), which can further activate the expression of NLRP3 and NF-κB signaling, ultimately promoting the release of inflammation (39,40). Evidence indicates that DOCK8 can activate STAT3 signaling in B cells (41). The same finding has been reported by Keles *et al* (38); that DOCK8 can interact with STAT3 and regulates its activation in T cells. The results of the present study showed that the enhanced contents of p-STAT3, NLRP3, ASC, caspase1 and p-p65 in Aβ-induced BV2 cells were decreased following interfering DOCK8 expression, implying that DOCK8 knockdown could inhibit the STAT3/NLRP3/NF-κB signaling pathway in Aβ-induced BV2 cells. The suppressive effects of DOCK8 silencing on the activation, inflammation, migration, invasion and polarization of Aβ-induced BV2 cells were reversed by Colivelin, indicating that DOCK8 interference repressed the malignant behaviors of Aβ-induced BV2 cells by blocking STAT3/NLRP3/NF-κB signaling. Furthermore, it was found that DOCK8 deficiency promoted the viability but repressed the apoptosis of Aβ-induced HT22 cells, implying that DOCK8 silencing helped to protect against hippocampal neuronal damage. Further mechanistic studies are needed to elucidate the interaction between Aß stimulation, DOCK8 and any subsequent pathway in the future experiments, which is a limitation of the present study.

In conclusion, the present study was the first, to the best of the authors' knowledge, to discuss the regulatory role DOCK8 in AD and uncover its detailed mechanism, which lays the foundation for the study of DOCK8 in neurodegenerative

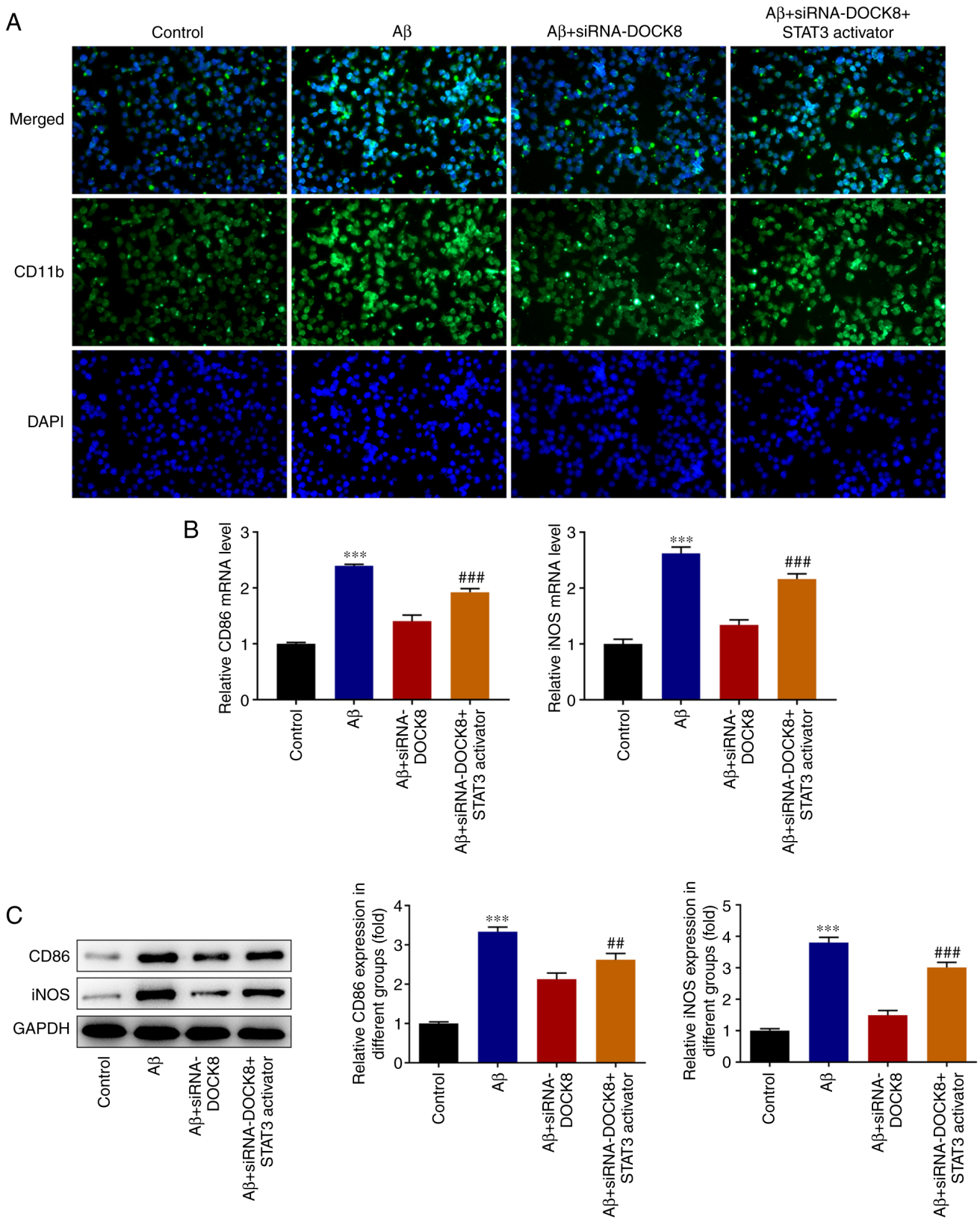

Figure 8. DOCK8 interference inhibits the polarization of Aβ-induced BV2 cells to M1 cells by suppressing STAT3/NLRP3/NF-κB signaling. (A) The expression of CD11b was detected using immunofluorescence staining. Magnification, x200. The expression levels of iNOS and CD86 using (B) reverse transcription-quantitative PCR and (C) western blotting. ***P<0.001 vs. control; $^{\#\#}$P<0.01, $^{\#\#\#}$P<0.001 vs. Aβ + siRNA-DOCK8. DOCK8, dedicator of cytokinesis 8; Aβ, amyloid β; NLRP3, NLR family pyrin domain containing 3; CD, cluster of differentiation; iNOS, inducible nitric oxide synthase; siRNA, short interfering RNA; NC, negative control.

diseases. However, there were also some limitations. For example, the role of DOCK8 in animal model and in clinic was not addressed in the present study; more studies need to be performed in the future.

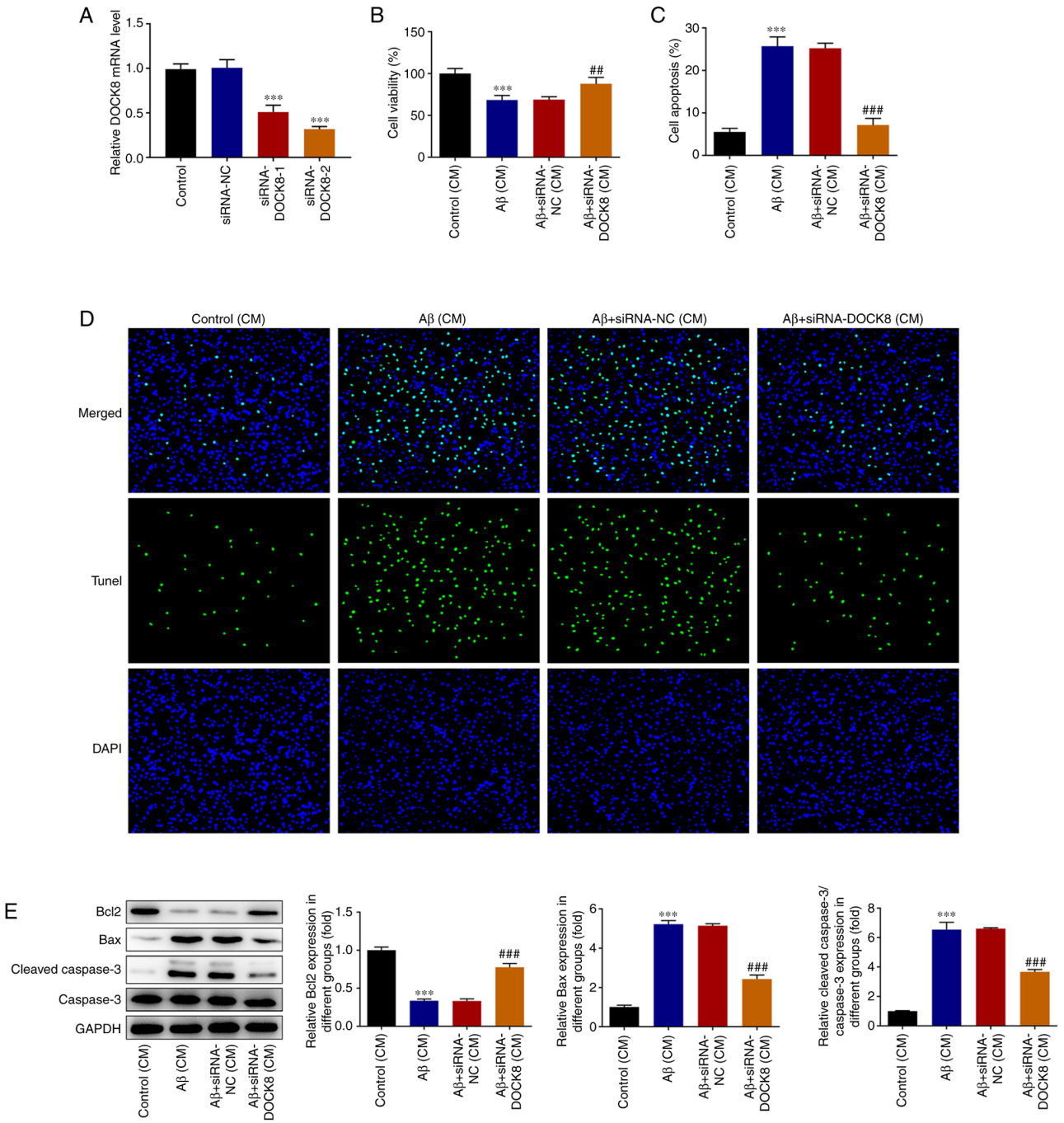

Figure 9. DOCK8 interference inhibits the neuronal activity damage and apoptosis of hippocampal HT22 cells induced by neuroinflammatory release in BV2 cells. (A) The transfection efficacy was detected using reverse transcription-quantitative PCR. ***P<0.001 vs. siRNA-NC. (B) The viability was detected using CCK-8. (C-D) The apoptosis was detected using terminal-deoxynucleotidyl transferase mediated nick end labeling. Magnification, x200. (E) The expression levels of apoptosis-related proteins were detected using western blotting. ***P<0.001 vs. control (CM); ##P<0.01, ###P<0.001 vs. Aβ + siRNA-NC (CM). DOCK8, dedicator of cytokinesis 8; siRNA, short interfering RNA; NC, negative control; CM, conditioned medium.

Acknowledgements

Not applicable.

Funding

This work was supported by Special Funds for Fundamental Research Expenses of Central Universities (grant nos. 2017KFYXJJ084 and 2018KFYYXJJ113).

Availability of data and material

The datasets used and/or analyzed during the current study are available from the corresponding author on reasonable request.

Ethics approval and consent to participate

Not applicable.

Patient consent for publication

Not applicable.

Authors' contributions

XZ and QW designed the study and performed the experiments. JH and DX performed the experiments and analyzed the data. XZ and SZ interpreted the data and drafted the manuscript. QW revised the manuscript for important intellectual content. All authors have read and approved the final manuscript. XZ and QW confirm the authenticity of all the raw data.

Competing interests

The authors declare that they have no competing interests.

References

1. Cui Y, Wang Y, Zhao D, Feng X, Zhang L and Liu C: Loganin prevents BV-2 microglia cells from Abeta1-42 -induced inflammation via regulating TLR4/TRAF6/NF-κB axis. Cell Biol Int 42: 1632-1642, 2018.
2. Lane CA, Hardy J and Schott JM: Alzheimer's disease. Eur J Neurol 25: 59-70, 2018.
3. De-Paula VJ, Radanovic M, Diniz BS and Forlenza OV: Alzheimer's disease. Subcell Biochem 65: 329-352, 2012.
4. Calsolaro V and Edison P: Neuroinflammation in Alzheimer's disease: Current evidence and future directions. Alzheimers Dement 12: 719-732, 2016.
5. Varnum MM and Ikezu T: The classification of microglial activation phenotypes on neurodegeneration and regeneration in Alzheimer's disease brain. Arch Immunol Ther Exp (Warsz) 60: 251-266, 2012.
6. Unger MS, Li E, Scharnagl L, Poupardin R, Altendorfer B, Mrowetz H, Hutter-Paier B, Weiger TM, Heneka MT, Attems J and Aigner L: CD8(+) T-cells infiltrate Alzheimer's disease brains and regulate neuronal- and synapse-related gene expression in APP-PS1 transgenic mice. Brain Behav Immun 89: 67-86, 2020.
7. Mosher KI and Wyss-Coray T: Microglial dysfunction in brain aging and Alzheimer's disease. Biochem Pharmacol 88: 594-604, 2014.
8. Kang SY, Jung HW, Lee MY, Lee HW, Chae SW and Park YK: Effect of the semen extract of Cuscuta chinensis on inflammatory responses in LPS-stimulated BV-2 microglia. Chin J Nat Med 12: 573-581, 2014.
9. Namekata K, Kimura A, Kawamura K, Harada C and Harada T: Dock GEFs and their therapeutic potential: Neuroprotection and axon regeneration. Prog Retin Eye Res 43: 1-16, 2014.
10. Kearney CJ, Randall KL and Oliaro J: DOCK8 regulates signal transduction events to control immunity. Cell Mol Immunol 14: 406-411, 2017.
11. Namekata K, Guo X, Kimura A, Arai N, Harada C and Harada T: DOCK8 is expressed in microglia, and it regulates microglial activity during neurodegeneration in murine disease models. J Biol Chem 294: 13421-13433, 2019.
12. Biggs CM, Keles S and Chatila TA: DOCK8 deficiency: Insights into pathophysiology, clinical features and management. Clin Immunol 181: 75-82, 2017.
13. Moon MY, Kim HJ, Li Y, Kim JG, Jeon YJ, Won HY, Kim JS, Kwon HY, Choi IG, Ro E, *et al*: Involvement of small GTPase RhoA in the regulation of superoxide production in BV2 cells in response to fibrillar Abeta peptides. Cell Signal 25: 1861-1869, 2013.
14. Cimino PJ, Yang Y, Li X, Hemingway JF, Cherne MK, Khademi SB, Fukui Y, Montine KS, Montine TJ and Keene CD: Ablation of the microglial protein DOCK2 reduces amyloid burden in a mouse model of Alzheimer's disease. Exp Mol Pathol 94: 366-371, 2013.
15. Jiang CQ, Ma LL, Lv ZD, Feng F, Chen Z and Liu ZD: Polydatin induces apoptosis and autophagy via STAT3 signaling in human osteosarcoma MG-63 cells. J Nat Med 74: 533-544, 2020.
16. Jian M, Kwan JS, Bunting M, Ng RC and Chan KH: Adiponectin suppresses amyloid-β oligomer (AβO)-induced inflammatory response of microglia via AdipoR1-AMPK-NF-κB signaling pathway. J Neuroinflammation 16: 110, 2019.
17. Livak KJ and Schmittgen TD: Analysis of relative gene expression data using real-time quantitative PCR and the 2(-Delta Delta C(T)) method. Methods 25: 402-408, 2001.
18. Latta CH, Brothers HM and Wilcock DM: Neuroinflammation in Alzheimer's disease; A source of heterogeneity and target for personalized therapy. Neuroscience 302: 103-111, 2015.
19. Heneka MT, Carson MJ, El Khoury J, Landreth GE, Brosseron F, Feinstein DL, Jacobs AH, Wyss-Coray T, Vitorica J, Ransohoff RM, *et al*: Neuroinflammation in Alzheimer's disease. Lancet Neurol 14: 388-405, 2015.
20. Heppner FL, Ransohoff RM and Becher B: Immune attack: The role of inflammation in Alzheimer disease. Nat Rev Neurosci 16: 358-372, 2015.
21. Imai Y, Ibata I, Ito D, Ohsawa K and Kohsaka S: A novel gene iba1 in the major histocompatibility complex class III region encoding an EF hand protein expressed in a monocytic lineage. Biochem Biophys Res Commun 224: 855-862, 1996.
22. Maneu V, Noailles A, Megias J, Gómez-Vicente V, Carpena N, Gil ML, Gozalbo D and Cuenca N: Retinal microglia are activated by systemic fungal infection. Invest Ophthalmol Vis Sci 55: 3578-3585, 2014.
23. Shi FJ, Xie H, Zhang CY, Qin HF, Zeng XW, Lou H, Zhang L, Xu GT, Zhang JF and Xu GX: Is Iba-1 protein expression a sensitive marker for microglia activation in experimental diabetic retinopathy? Int J Ophthalmol 14: 200-208, 2021.
24. Muhammad T, Ikram M, Ullah R, Rehman SU and Kim MO: Hesperetin, a citrus flavonoid, attenuates LPS-induced neuroinflammation, apoptosis and memory impairments by modulating TLR4/NF-κB signaling. Nutrients 11: 648, 2019.
25. Park T, Chen H, Kevala K, Lee JW and Kim HY: N-Docosahexaenoylethanolamine ameliorates LPS-induced neuroinflammation via cAMP/PKA-dependent signaling. J Neuroinflammation 13: 284, 2016.
26. Zhu SH, Liu BQ, Hao MJ, Fan YX, Qian C, Teng P, Zhou XW, Hu L, Liu WT, Yuan ZL and Li QP: Paeoniflorin suppressed high glucose-induced retinal microglia MMP-9 expression and inflammatory response via inhibition of TLR4/NF-κB pathway through upregulation of SOCS3 in diabetic retinopathy. Inflammation 40: 1475-1486, 2017.
27. Hopperton KE, Mohammad D, Trepanier MO, Giuliano V and Bazinet RP: Markers of microglia in post-mortem brain samples from patients with Alzheimer's disease: A systematic review. Mol Psychiatry 23: 177-198, 2018.
28. Dobryakova YV, Kasianov A, Zaichenko MI, Stepanichev MY, Chesnokova EA, Kolosov PM, Markevich VA and Bolshakov AP: Intracerebroventricular administration of (192)IgG-Saporin alters expression of microglia-associated genes in the dorsal but not ventral hippocampus. Front Mol Neurosci 10: 429, 2017.
29. Aydin SE, Kilic SS, Aytekin C, Kumar A, Porras O, Kainulainen L, Kostyuchenko L, Genel F, Kütükcüler N, Karaca N, *et al*: DOCK8 deficiency: Clinical and immunological phenotype and treatment options-a review of 136 patients. J Clin Immunol 35: 189-198, 2015.
30. Zhang Z, Bao Y, Zhou L, Ye Y, Fu W and Sun C: DOCK8 Serves as a prognostic biomarker and is related to immune infiltration in patients with HPV positive head and neck squamous cell carcinoma. Cancer Control 28: 10732748211011951, 2021.
31. Xu X, Han L, Zhao G, Xue S, Gao Y, Xiao J, Zhang S, Chen P, Wu ZY, Ding J, *et al*: LRCH1 interferes with DOCK8-Cdc42-induced T cell migration and ameliorates experimental autoimmune encephalomyelitis. J Exp Med 214: 209-226, 2017.
32. Miyamoto Y, Torii T, Kawahara K, Tanoue A and Yamauchi J: Dock8 interacts with Nck1 in mediating Schwann cell precursor migration. Biochem Biophys Rep 6: 113-123, 2016.
33. Ham H, Guerrier S, Kim J, Schoon RA, Anderson EL, Hamann MJ, Lou Z and Billadeau DD: Dedicator of cytokinesis 8 interacts with talin and Wiskott-Aldrich syndrome protein to regulate NK cell cytotoxicity. J Immunol 190: 3661-3669, 2013.
34. Hillmer EJ, Zhang H, Li HS and Watowich SS: STAT3 signaling in immunity. Cytokine Growth Factor Rev 31: 1-15, 2016.
35. Takeda K, Kaisho T, Yoshida N, Takeda J, Kishimoto T and Akira S: Stat3 activation is responsible for IL-6-dependent T cell proliferation through preventing apoptosis: Generation and characterization of T cell-specific Stat3-deficient mice. J Immunol 161: 4652-4660, 1998.

36. Kortylewski M and Yu H: Role of Stat3 in suppressing anti-tumor immunity. Curr Opin Immunol 20: 228-233, 2008.
37. Egwuagu CE: STAT3 in $CD4^+$ T helper cell differentiation and inflammatory diseases. Cytokine 47: 149-156, 2009.
38. Keles S, Charbonnier LM, Kabaleeswaran V, Reisli I, Genel F, Gulez N, Al-Herz W, Ramesh N, Perez-Atayde A, Karaca NE, *et al*: Dedicator of cytokinesis 8 regulates signal transducer and activator of transcription 3 activation and promotes TH17 cell differentiation. J Allergy Clin Immunol 138: 1384-1394 e1382, 2016.
39. Zhu H, Jian Z, Zhong Y, Ye Y, Zhang Y, Hu X, Pu B, Gu L and Xiong X: Janus kinase inhibition ameliorates ischemic stroke injury and neuroinflammation through reducing NLRP3 inflammasome activation via JAK2/STAT3 pathway inhibition. Front Immunol 12: 714943, 2021.
40. Dai R, Jiang Q, Zhou Y, Lin R, Lin H, Zhang Y, Zhang J and Gao X: Lnc-STYK1-2 regulates bladder cancer cell proliferation, migration, and invasion by targeting miR-146b-5p expression and AKT/STAT3/NF-kB signaling. Cancer Cell Int 21: 408, 2021.
41. Pal M, Bao W, Wang R, Liu Y, An X, Mitchell WB, Lobo CA, Minniti C, Shi PA, Manwani D, *et al*: Hemolysis inhibits humoral B-cell responses and modulates alloimmunization risk in patients with sickle cell disease. Blood 137: 269-280, 2021.